Supporting Information

Carbon aerogels with atomic dispersion of binary iron-cobalt sites as effective oxygen catalysts for flexible zinc-air batteries

Yang Chen,[a] Shengqiang Hu,[b] Forrest Nichols,[c] Frank Bridges,[d] Shuting Kan,[a] Ting He,[a,*] Yi Zhang[a,*] and Shaowei Chen,[c,*]

[a] College of Chemistry and Chemical Engineering, Central South University, Changsha, Henan 410083, China

[b] State Key Laboratory for the Chemistry and Molecular Engineering of Medicinal Resources, College of Chemistry and Pharmacy, Guangxi Normal University, Guilin, Guangxi 541004, China

[c] Department of Chemistry and Biochemistry, University of California, 1156 High Street, Santa Cruz, CA 95064, USA

[d] Department of Physics, University of California, 1156 High Street, Santa Cruz, CA 95064, USA

Table S1. Porosity of NCAG/Fe-Co, NCAG/Fe, and NCAG/Co samples.

Sample	S_{BET} (m^2 g^{-1})	Pore volumes (cm^3 g^{-1})	Micropore (%)	Mesopore (%)	Macropore (%)
NCAG/Fe-Co	748.2	0.84	32.1	66.7	1.2
NCAG/Co	822.7	1.05	25.7	72.4	1.9
CACG/Fe	893.3	1.15	27.8	69.6	2.6

Table S2. Metal contents determined by ICP-OES measurements.

Sample	Fe (wt.%)	Co (wt.%)
NCAG/Fe	0.6	
NCAG/Fe-Co	0.7	1.1
NCAG/Co		1.0

Table S3. Elemental contents of the various catalysts determined by XPS.

Sample	C (wt.%)	O (wt.%)	N (wt.%)	Fe (wt.)%	Co (wt.%)
NCAG/Fe	89.0	5.9	4.1	1.0	
NCAG/Fe-Co	89.3	4.8	5.0	0.9	1.0
NCAG/Co	89.4	4.7	4.6		1.3

Table S4. Binding energies and contents of various nitrogen dopants in the series of carbon aerogels.

Sample	pridinic N	M-N	graphitic N
NCAG/Fe	398.14 eV	**398.80 eV**	401.02 eV
	0.4 wt.%	0.8 wt.%	2.9 wt.%
NCAG/Fe-Co	398.16 eV	**398.86 eV**	401.00 eV
	0.4 wt.%	1.4 wt.%	3.2 wt.%
NCAG/Co	398.25 eV	**399.03 eV**	401.07 eV
	0.5 wt.%	1.1 wt.%	2.9 wt.%

Table S5. Binding energies of Co and Fe 2p electrons in the series of carbon aerogels.

Sample	Co (eV)	Fe^{2+} (eV)	Fe^{3+} (eV)
NCAG/Fe-Co	780.4	710.5	715.0
NCAG/Fe		710.0	714.7
NCAG/Co	780.6		

Table S6 EXAFS fitting results of FePc.

Bond	Coordination number	r (Å)	σ^2 (Å^2)
Fe-N	4	1.962	0.0052
Fe-C	8	2.985	0.0045
Fe-N	4	3.214	0.0036

Table S7 Atomic positions of FeN_3CoN_3 as depicted in Figure 3d.

Atom	*x*	*y*	*z*
Fe	0	0	0
N	-1.803	0	0
Co	2.787	0	0
N	0	1.947	0
N	0	-1.947	0
N	1.75	0	1.64
N	1.75	0	-1.64
N	4.59	0	0

Table S8. EXAFS fitting results of NCAG/Fe-Co.

Bond	Coordination number	r (Å)	σ^2 (Å^2)
Fe-N_1	1	1.803	0.0013
Fe-N_2	2	1.947	0.0015
Fe-N_3	2	2.394	0.0017
Fe-Co	1	2.787	0.0023

Table S9. Comparison of the performance of flexible Zn-air batteries based on relevant oxygen cayalsts.

Catalyst	Power density (mW cm^{-2})	OCV (V)	Ref.
NCAG/FeCo	117	1.47	This work
N-doped Ni_2CoO_4	30		1
FeCoNi/carbon nanotube	85	1.45	2
Fe-Co_4N@N-C	72	1.34	3
Co_3O_4/carbon fiber		1.33	4
FeCo alloy/N-carbon	98	1.25	5
Zn, Co-N_x-C-S_y	15	1.56	6
Co/carbon nanotube	63	1.34	7

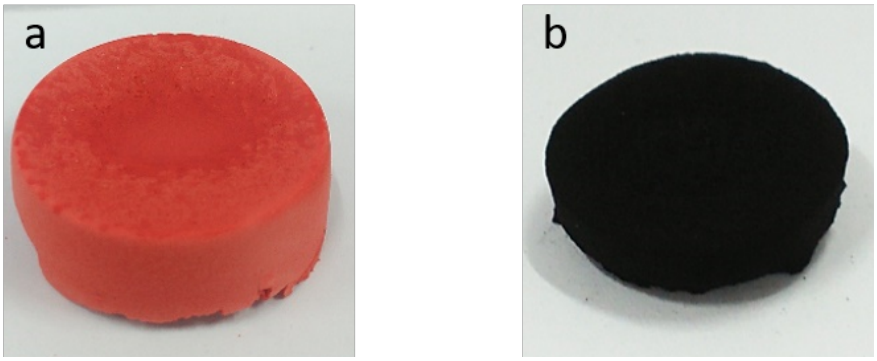

Figure S1. Digital photos of (a) freeze-dried $G_{Si\text{-}Zn}$/Fe@CoPM hydrogel and (b) NCAG/Fe-Co aerogel.

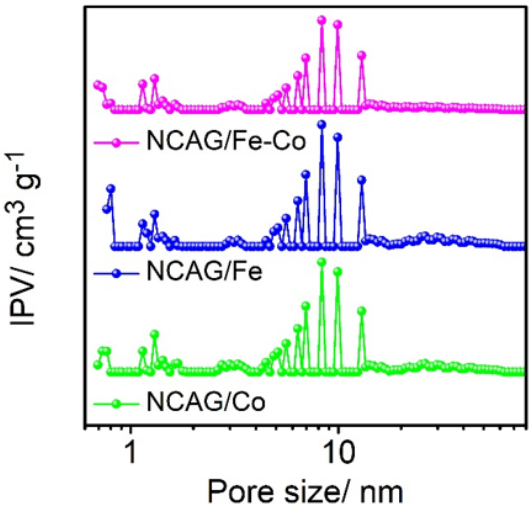

Figure S2. Pore-size distributions of NCAG/Fe-Co, NCAG/Fe, and NCAG/Co.

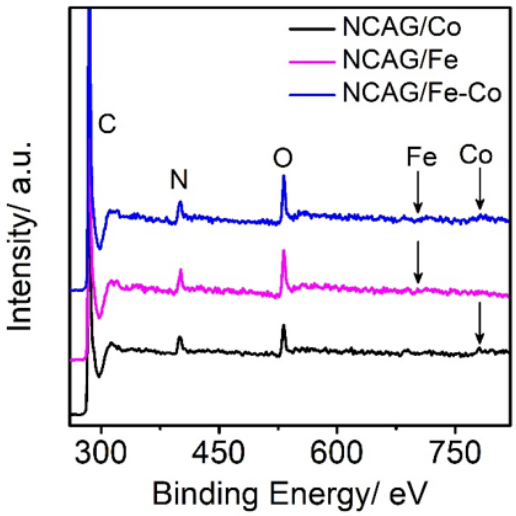

Figure S3. XPS survey spectra of NCAG/Co, NCAG/Fe, and NCAG/Fe-Co.

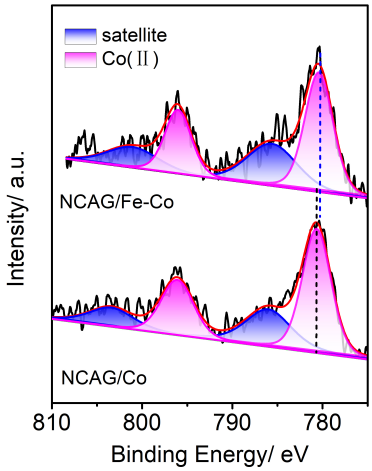

Figure S4. High-resolution XPS scan of the Co 2p electrons of NCAG/Fe-Co and NCAG/Co. Black curves are experimental data and shaded peaks are deconvolution fits.

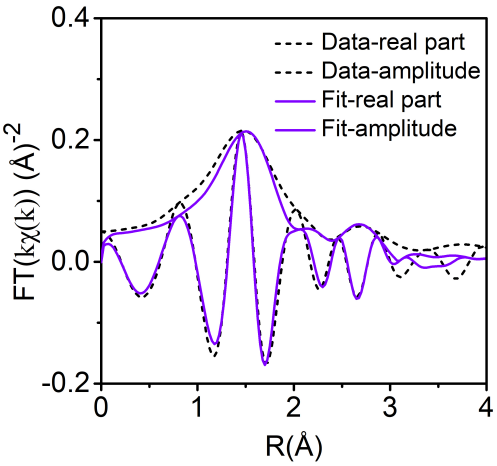

Figure S5 Fe K-edge EXFAS of FePc and the fitting curve. The fitting result is summarized in Table S6.

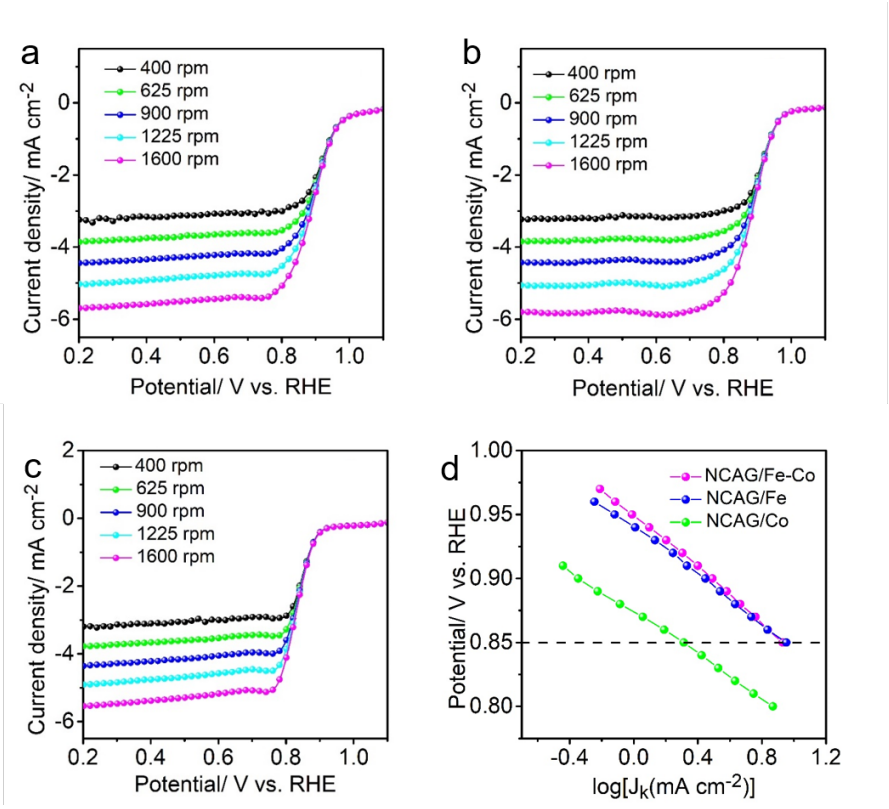

Figure S6. (a-c) ORR polarization curves of (a) NCAG/Fe-Co, (b) NCAG/Fe, and (c) NCAG/Co at various rotation speeds and (d) the corresponding Tafel plots.

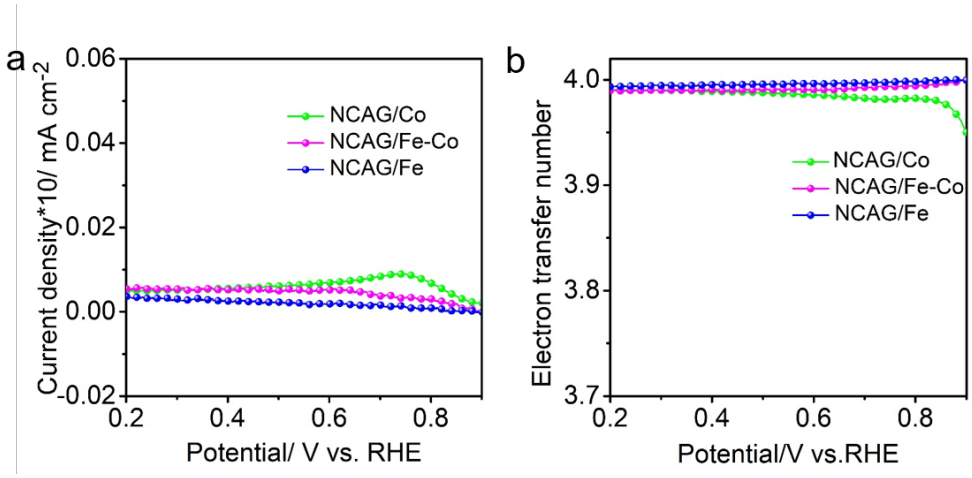

Figure S7. (a) Current density at the ring electrode during RRDE measurements, and (b) electron transfer number of NCAG/Co, NCAG/Fe, and NCAG/Fe-Co.

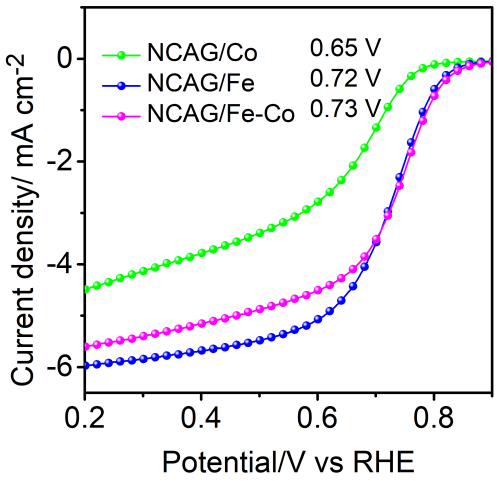

Figure S8. LSV curves of the ORR catalysts at 1600 rpm and 5 mV s^{-1} in 0.1 $HClO_4$. The half-wave potentials ($E_{1/2}$) of NGCA/Co, NGCA/Fe and NGCA/Fe-Co are +0.65, +0.72 and +0.73 V, respectively.

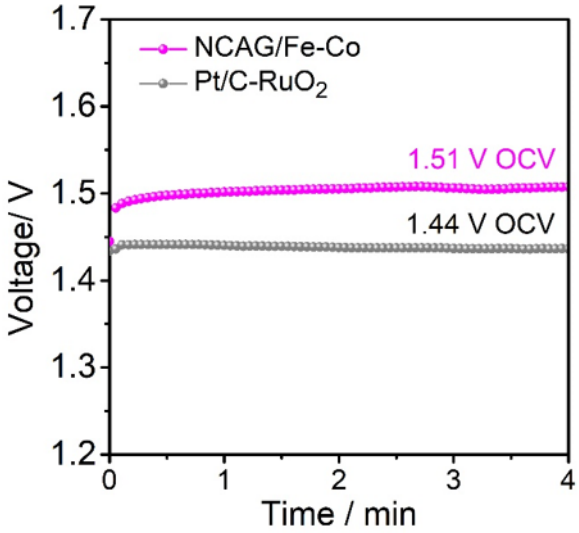

Figure S9. Open circuit voltage of liquid Zn-air battery using either NCAG/Fe-Co or Pt/C-RuO_2 mixture as the cathode catalyst.

References

1 J. Bian, X. Cheng, X. Meng, J. Wang, J. Zhou, S. Li, Y. Zhang and C. Sun, *ACS Appl. Energy Mater.*, 2019, **2**, 2296-2304.

2 Z. Wang, J. Ang, B. Zhang, Y. Zhang, X. Y. D. Ma, T. Yan, J. Liu, B. Che, Y. Huang and X. Lu, *Appl. Catal., B*, 2019, **254**, 26-36.

3 Q. Xu, H. Jiang, Y. Li, D. Liang, Y. Hu and C. Li, *Appl. Catal., B*, 2019, **256**, 117893.

4 X. Chen, B. Liu, C. Zhong, Z. Liu, J. Liu, L. Ma, Y. Deng, X. Han, T. Wu and W. Hu, *Adv. Energy Mater.*, 2017, **7**, 1700779.

5 C.-Y. Su, H. Cheng, W. Li, Z.-Q. Liu, N. Li, Z. Hou, F.-Q. Bai, H.-X. Zhang and T.-Y. Ma, *Adv. Energy Mater.*, 2017, **7**, 1602420.

6 D. Liu, B. Wang, H. Li, S. Huang, M. Liu, J. Wang, Q. Wang, J. Zhang and Y. Zhao, *Nano Energy*, 2019, **58**, 277-283.

7 D. Ji, L. Fan, L. Li, N. Mao, X. Qin, S. Peng and S. Ramakrishna, *Carbon*, 2019, **142**, 379-387.